



# Impact of sequence type and field strength (1.5, 3, and 7T) on 4D flow MRI hemodynamic aortic parameters in healthy volunteers

Stephanie Wiesemann<sup>1,2</sup> | Sebastian Schmitter<sup>3</sup>  | Aylin Demir<sup>1</sup> | Marcel Prothmann<sup>1</sup> | Carsten Schwenke<sup>4</sup> | Ashish Chawla<sup>5</sup> | Florian von Knobelsdorff-Brenkenhoff<sup>1,6</sup> | Andreas Greiser<sup>7</sup> | Ning Jin<sup>8</sup> | Emilie Bollache<sup>9</sup> | Michael Markl<sup>10</sup> | Jeanette Schulz-Menger<sup>1,2</sup> 

<sup>1</sup>Department of Cardiology and Nephrology, Experimental and Clinical Research Center, a joint cooperation between the Charité Medical Faculty and the Max-Delbrueck Center for Molecular Medicine and HELIOS Hospital Berlin Buch, Berlin, Germany

<sup>2</sup>DZHK (German Center for Cardiovascular Research), partner site Berlin, Berlin, Germany

<sup>3</sup>Physikalisch-Technische Bundesanstalt (PTB), Braunschweig and Berlin, Germany

<sup>4</sup>SCO:SSIS Statistical Consulting, Berlin, Germany

<sup>5</sup>Khoo Teck Puat Hospital, Yishun Central, Singapore, Singapore

<sup>6</sup>Clinic Agatharied, Department of Cardiology, Ludwig-Maximilians-University Munich, Hausham, Germany

<sup>7</sup>Siemens Healthcare, Erlangen, Germany

<sup>8</sup>Siemens Medical Solutions, Columbus, Ohio, USA

<sup>9</sup>Sorbonne Université, CNRS, INSERM, Laboratoire d'Imagerie Biomédicale, LIB, Paris, France

<sup>10</sup>Department of Radiology, Northwestern University, Feinberg School of Medicine, Chicago, Illinois, USA

## Correspondence

Jeanette Schulz-Menger, Department of Cardiology and Nephrology, Experimental and Clinical Research Center, a joint cooperation between the Charité Medical Faculty and the Max-Delbrueck Center for Molecular Medicine and HELIOS Hospital Berlin Buch, Lindenbergerweg 80, 13125 Berlin, Germany.  
Email: jeanette.schulz-menger@charite.de

**Purpose:** 4D flow magnetic resonance imaging (4D-MRI) allows time-resolved visualization of blood flow patterns, quantification of volumes, velocities, and advanced parameters, such as wall shear stress (WSS). As 4D-MRI enters the clinical arena, standardization and awareness of confounders are important. Our aim was to evaluate the equivalence of 4D flow-derived aortic hemodynamics in healthy volunteers using different sequences and field strengths.

**Methods:** 4D-MRI was acquired in 10 healthy volunteers at 1.5T using three different prototype sequences, at 3T and at 7T (Siemens Healthineers). After evaluation of diagnostic quality in three segments (ascending-, descending aorta, aortic arch), peak velocity, flow volumes, and WSS were investigated. Equivalence limits for comparison of field strengths/sequences were based on the limits of Bland-Altman analyses of the intraobserver variability.

**Results:** Non-diagnostic quality was found in 10/144 segments, 9/10 were obtained at 7T. Apart for the comparison of forward flow between sequence 1 and 3, the differences in measurements between field strengths/sequences exceeded the range of agreement. Significant differences were found between field strengths/sequences for

forward flow (1.5T vs. 3T, 3T vs. 7T, sequence 1 vs. 3, 2 vs. 3 [ $P < .001$ ]), WSS (1.5T vs. 3T [ $P < .05$ ], sequence 1 vs. 2, 1 vs. 3, 2 vs. 3 [ $P < .001$ ]), and peak velocity (1.5T vs. 7T, sequence 1 vs. 3 [ $P > .001$ ]). All parameters at all field strengths/with all sequences correlated moderately to strongly ( $r \geq 0.5$ ).

**Conclusion:** Data from all sequences could be acquired and resulting images showed sufficient quality for further analysis. However, the variability of the measurements of peak velocity, flow volumes, and WSS was higher when comparing field strengths/sequences as the equivalence limits defined by the intraobserver assessments.

#### KEYWORDS

4D flow, 7T, aorta, cardiovascular magnetic resonance imaging, non-invasive hemodynamics, standardization

## 1 | INTRODUCTION

4D flow has been shown to be a promising tool in cardiovascular MRI for the non-invasive evaluation of hemodynamics in adult and pediatric cardiology.<sup>1-3</sup> It can provide both time-resolved visualization of complex flow patterns and quantification of flow velocities and volumes. Furthermore, more advanced parameters such as wall shear stress (WSS) can be derived.<sup>4</sup>

Currently, only a few markers obtained by echocardiography or cardiovascular MRI mainly based on the aortic shape and size help with the decision on the timing and type of surgery in patients with aortic valve pathology and/or aortic aneurysm.<sup>5,6</sup>

WSS has shown to have great potential in this field as several studies have shown the additional benefit of determining the WSS in different patients with aortic valve pathologies or pathologies of the thoracic aorta.<sup>7-15</sup> It was shown that hemodynamics were altered in the ascending aorta in the presence of an aortic valve stenosis. Such alterations included a local increase in WSS and were related to stenosis severity.<sup>9,16</sup> It was also observed that flow patterns were altered and WSS was regionally elevated in the ascending aorta of patients after aortic valve replacement.<sup>17,18</sup> First follow-up studies have been conducted to evaluate changes in hemodynamics or WSS over time in specific pathologies or after surgery and 4D flow MRI was able to show the longitudinal evolution of already initially abnormal WSS values.<sup>19,20</sup> Therefore, 4D flow may help with therapy guiding and decision making by providing additional and potentially complementary information.

Since initial studies have demonstrated that certain types of 4D flow scans can be obtained in about 2 min,<sup>21,22</sup> the implementation of 4D flow in clinical routine is imminent. However, to reach a broad application in clinical routine, standardization and awareness of confounders are essential. Thus, the aim of our study was to evaluate the equivalence of 4D flow MRI-derived aortic hemodynamic parameters at three different field strengths (1.5T, 3T, and 7T). Additionally, we analyzed the equivalence of three different sequence variants at 1.5T.

## 2 | METHODS

The study included 10 healthy volunteers without any known cardiovascular risk factors or history of cardiac diseases as well as normal left ventricular (LV) function and a tricuspid aortic valve without stenosis or insufficiency as assessed by cardiovascular MRI. Approval of the local Institutional Review Board and informed consent from each participant were obtained.

### 2.1 | Image acquisition

Each volunteer was scanned three times; in each of these sessions the volunteer was scanned at a single field strength: 1.5T (Magnetom Avanto fit), 3T (Magnetom Verio), and 7T (Magnetom 7T, whole-body research scanner) (all Siemens Healthcare, Erlangen, Germany). At 7T, a local single-channel transmit, 16-channel receive radio-frequency transceiver array was used, which provided an optimized transmit magnetic field pattern within the heart.<sup>23</sup> At 3T, a 32-channel receiver coil and, at 1.5T, an 18-channel anterior surface coil and 12 elements of the spine coil were used. The acquisition volume was defined over the entire thoracic aorta down to the diaphragm. For cardiac gating electrocardiograph (ECG) was used. Due to the magneto-hydrodynamic effect, which increasingly impacts the ECG signal with increasing field strength, we used an acoustic cardiac triggering system (ACT, Easy ACT, MRI.TOOLS GmbH, Berlin Germany) at 7T when ECG detection failed.<sup>24</sup> Data acquisition was performed during free breathing using a respiratory navigator placed on the lung-liver interface.

At 1.5T, three prototype 4D flow sequence variants using different scan parameters were applied as listed in Table 1. These three sequence variants were acquired within one scanning session. Parameters for the sequences used at 3T and 7T are also listed in Table 1. The 4D flow sequences were

**TABLE 1** Sequence parameters for the three different sequences at 1.5T as well as for 3T and 7T

Field strength (sequence)	1.5T (sequence 1)	1.5T (sequence 2)	1.5T (sequence 3)	3T	7T
TE in ms	2.4	2.3	2.3	2.6	2.4
TR in ms <sup>#</sup>	39.2	38.9	38.9	40.8	38.4
Bandwidth in Hz/pixel	450	496	496	450	450
GRAPPA	R = 5	R = 2	R = 2	R = 5	R = 2
Nominal flip angle in degrees	8	8	8	7	10 <sup>##</sup>
Field of view in mm <sup>3</sup>	270-292 × 360 × 62.5 <sup>*</sup>	252-270 × 360 × 62.5 <sup>*</sup>	270-292 × 360 × 62.5 <sup>*</sup>	270 × 360 × 83.2	292 × 360 × 38.4
Acquisition matrix (phase encode × readout × slice)	70-90 × 160 × 26	78-91 × 160 × 18	84-91 × 160 × 18	100 × 160 × 32	88 × 160 × 26
Acquired voxel size in mm <sup>3</sup> (phase encode × readout × slice)	3.3-3.9 × 2.3 × 2.4 <sup>**</sup>	3.2 × 2.3 × 3.5	3.2 × 2.3 × 3.5	2.7 × 2.3 × 2.6	3.3 × 2.3 × 2.4
Reconstructed voxel size in mm <sup>3</sup> (phase encode × readout × slice)	2.3 × 2.3 × 2.4	2.3 × 2.3 × 2.4	2.3 × 2.3 × 2.4	2.7 × 2.3 × 2.6	2.3 × 2.3 × 2.4
Number of cardiac phases	20	18	25	18	20
Velocity encoding in m/s	1.5	1.5	1.5	1.5	1.5
ECG-gating	prospective	prospective	retrospective	prospective	prospective
Radiofrequency coil (receive channels)	30	30	30	32	16
Acquisition time mean ± SD in min	6.7 ± 1.8	8.5 ± 1.4	8.4 ± 1.5	9.0 ± 1.7	11.2 ± 3.0
Heart rate in beats/min	68.5 ± 8.3	67 ± 8.0	69 ± 8.1	70.4 ± 8.7	60 ± 10.8 <sup>+</sup>

Abbreviations: TE, echo time; TR, temporal resolution; GRAPPA, GeneRalized Autocalibrating Partial Parallel Acquisition; R, acceleration factor; ECG, electrocardiographic.

\*The field of view in phase encoding direction was adjusted to the subject's anatomy.

\*\*In two subjects the acquired pixel spacing along the phase encoding axis was increased to 3.9 mm.

#A twofold temporal segmentation factor has been used for all scans.

##The actual flip angle throughout the region of interest varies strongly at 7T.

+The heart rate at 7T is biased by the partially unreliable ECG detection, which may lead to lower heart rates.

selected based on their clinical availability to best represent a routine clinical setting.

Acquisition times for all sequences as well as the heart rates, which were retrospectively obtained from the Digital Imaging and Communications in Medicine (DICOM) data, are also provided in Table 1. Scan time was the longest at 7T, but varied substantially between approximately 8 and 15 min. The reason for such a large range is given by the navigator that failed in 5 of 10 subjects at 7T due to insufficient  $B_1^+$  magnitude to detect the position of the diaphragm. In these subjects the scan efficiency was 100% while the minimal efficiency of 56% was determined for the longest 7T scan. A sandbag was placed on the stomach to minimize respiratory motion. Scan sessions at 1.5T, 3T, and 7T took place within weeks. The first and second scan sessions were performed within  $4.2 \pm 3$  wk ( $29.3 \pm 21.1$  days), while the second and the third scan sessions were performed within  $2.8 \pm 1.6$  wk ( $19.6 \pm 10.9$  days). For each 4D flow scan, the heart rate was recorded. Additionally, at 3T, steady state free precession (SSFP) cine images for the evaluation of left ventricular function and assessment of the aortic valve were acquired. If significant artifacts occurred, gradient echo sequences were added.

## 2.2 | Analysis of 4D flow data

The image quality of 4D flow data was evaluated for each subject and for each sequence in magnitude images as well as in streamline visualization (Supporting Information Video S1, which is available online) in three contiguous segments: the ascending aorta, the aortic arch, and the descending aorta. The ascending aorta was defined from the aortic valve to proximal of the brachiocephalic trunk, the aortic arch ended at the aortic isthmus, and the descending aorta ended at the diaphragm. Image quality was graded as published before: 0 = non-diagnostic, 1 = good, 2 = excellent.<sup>25</sup> Non-diagnostic quality was defined as presence of artifacts, blurriness, or signal loss across or inside an aortic segment. Good quality was defined as the lack thereof, but challenging delineation or missing supra-aortic branches. In images with excellent quality, the aorta as well as the supra-aortic branches could be easily delineated, no blurriness or artifacts occurred. Segments with non-diagnostic quality were excluded from further analyses.

All remaining segments were analyzed for flow volumes, as well as WSS and peak velocity.<sup>4,19,26</sup>

Data were corrected online for Maxwell terms. Background velocities were corrected in MATLAB (The MathWorks Inc., USA) by fitting linear spatial gradients to the phase of static tissue, which was subtracted from the velocity data.<sup>27</sup> Subsequently, manual segmentation of the aorta was performed (Mimics, Materialise, Belgium). Then, 3D blood flow visualization and manual positioning of 2D planes for flow quantification were conducted (EnSight, Version 10.0, CEI, Apex, NC, USA). Nine cross-sectional planes were positioned perpendicularly to the longitudinal axis of the aortic wall as follows (Figure 1A): in the left ventricular outflow tract (P1), at the level of the sinotubular junction (P2), in the mid-ascending aorta (P3), proximal to the brachiocephalic trunk (P4), between the brachiocephalic trunk and the left common carotid artery (P5), between the left common carotid artery and the left subclavian artery (P6), at the aortic isthmus (P7), in the descending aorta after the isthmus (P8), and in the descending aorta at the level of P2 (P9). Flow within each plane was computed automatically.

3D WSS was calculated using a previously published approach.<sup>19,26</sup> Briefly, 3D WSS was calculated throughout the entire thoracic aortic wall at peak systole and the two previous and following cardiac time frames, peak systole being defined as the time frame with the highest velocity averaged over the whole aortic volume (MATLAB, The MathWorks Inc., USA). Peak systolic WSS values were then averaged over those five time frames and extracted in 10 segments throughout the thoracic aorta as defined in Figure 1B.

Finally, peak velocities were obtained from velocity maximum intensity projections in the ascending aorta, the aortic arch, and the descending aorta (Figure 1C) (MATLAB, The MathWorks Inc., Natick, MA, USA).<sup>28</sup>

### 2.3 | Statistical analysis

To account for the confounding effect of GRAPPA acceleration and prospective vs. retrospective ECG gating, field strength comparison between 1.5T and 3T considered 1.5T sequence 1, while comparison between 1.5T and 7T additionally considered 1.5T sequence 2.

A Wilcoxon signed-rank test was applied to test for statistically significant differences. Correlation was tested by Spearman rho's correlation. A moderate correlation was defined as  $r \geq 0.50$ , a strong correlation as  $r \geq 0.75$ .

Comparisons were performed using both the entire aorta and the ascending aorta only, since most abnormal findings in diseased patients are found in that region.

Results are reported for both, all 10 volunteers as well as only those who could be examined at all field strengths.

A subset of the data consisting of all field strengths and sequences was analyzed twice by one observer for intraobserver analysis. The time interval between the first and the second analysis was 9 mo. Bland-Altman analyses were used to assess the intraobserver variability and to set limits of agreement (95% confidence interval [CI] of difference) and

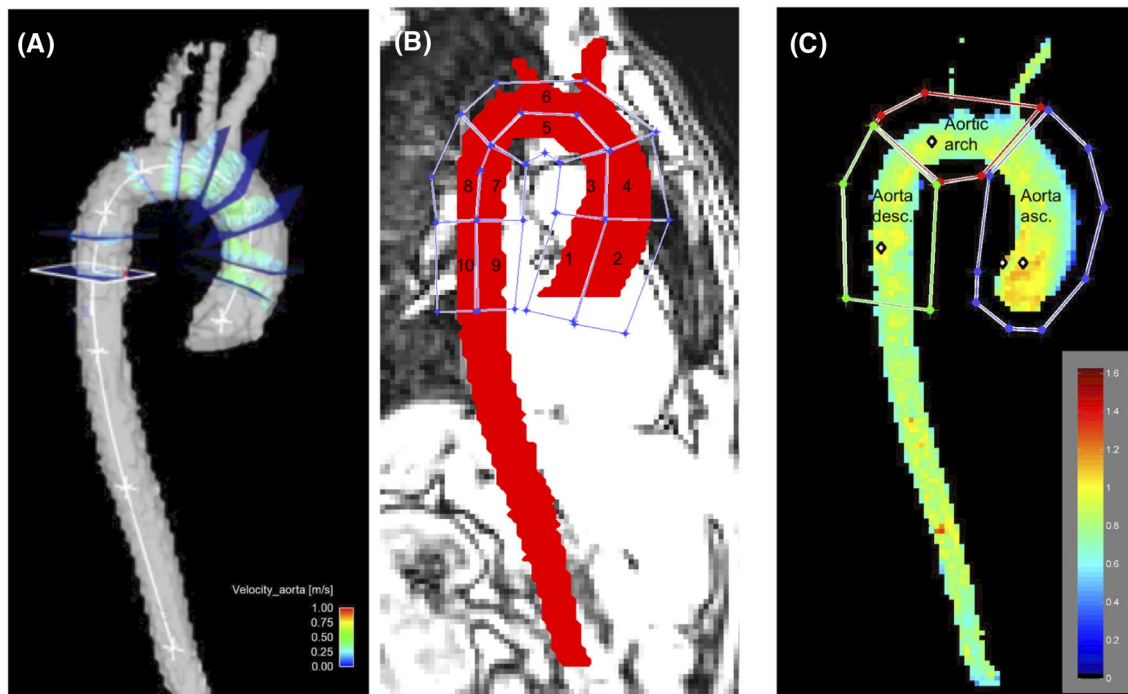


**FIGURE 1** Visualization of the locations used for quantitative assessment in the thoracic aorta: flow was evaluated in nine cross-sectional planes (A), WSS was evaluated in 10 wall regions (B), peak velocity was evaluated in the ascending aorta, the aortic arch, and the descending aorta (C)

range of agreement for each aortic parameter, which was used as equivalence range for the comparison of field strengths and sequences for each aortic parameter: equivalence was reached if the limits of the 95% CI of the difference between sequences laid within the limits of the 95% CI defined by the intraobserver analysis.

A subset of data including all sequences and field strengths was used for interobserver analysis. Agreement between the observer was assessed using intraclass correlation coefficient (ICC) and Bland-Altman analysis.

Statistical analysis was performed with SAS 9.4 (SAS Institute Inc., Cary, North Carolina, USA) and Graph Pad Prism 6.0 (GraphPad Software Inc., San Diego, California, USA). Graphics were created using Graph Pad Prism and plug-in software for MATLAB.

### 3 | RESULTS

Demographics of the 10 volunteers (6 female, mean age:  $33 \pm 9$  y) are provided in Table 2. Across the study cohort the averaged heart rate was  $67.7 \pm 8.7$  beats/min with no significant differences between the different 4D flow scans.

While at 1.5T and 3T all scans could be completed, at 7T, two sessions could not be performed due to technical problems with the hardware of the scanner. For cardiac gating, we used ACT in one volunteer at 7T, ECG was used in all other scans.

**TABLE 2** Baseline characteristics of the healthy volunteers.

n = 10 (6 f/4 m)	Mean $\pm$ SD
Age (yrs)	$33 \pm 8.9$
Height (cm)	$170.9 \pm 10.1$
Weight (kg)	$65.2 \pm 10$
BMI ( $\text{kg}/\text{m}^2$ )	$22.2 \pm 1.7$
LV-EF (%)	$63 \pm 5$

BSA = body-surface-area, LV = left ventricular, EF = ejection fraction.

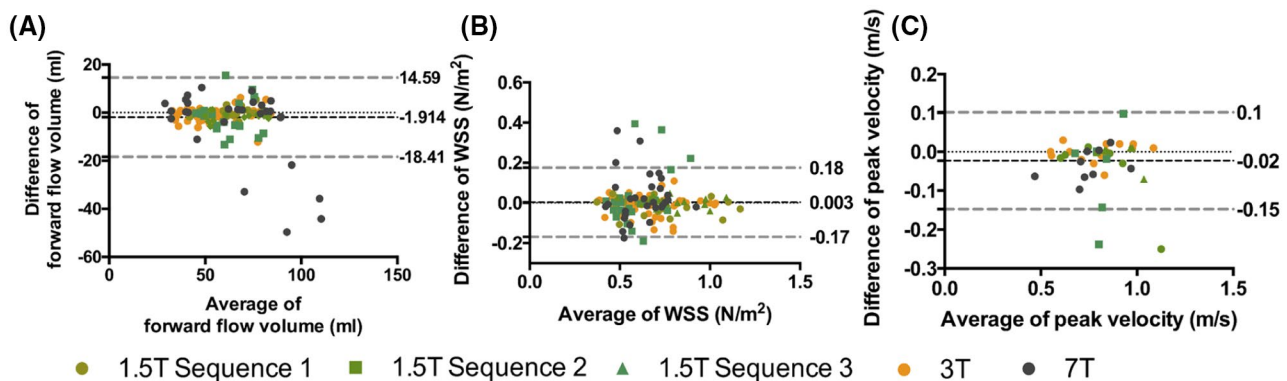


**FIGURE 2** Bland Altman analyses for intraobserver analysis of forward flow volume (A), WSS (B), and peak velocity (C). Each field strength is coded in a different color. The three sequences at 1.5T are additionally coded using a different shape

### 3.1 | Image quality

In total, 144 aortic segments were evaluated for image quality. Non-diagnostic quality was found in 10 segments (7%) (quality score = 0), 15 (10%) were scored as good (quality score = 1). The remaining 119 (83%) had excellent quality. Of the 10 segments with non-diagnostic image quality, 9 were obtained at 7T: 5 of them were located in the aortic arch, 4 of them in the descending aorta. The remaining segment was obtained during a scan with sequence 1 at 1.5T and was in the aortic arch. Among the 15 segments with good quality, 9 were found in the aortic arch (3 with sequence 1 at 1.5T, 2 with sequence 3 at 1.5T, 3 at 3T, and 1 at 7T), three segments were in the ascending aorta (1 with sequence 1 at 1.5T, and 2 at 3T), and three in the descending aorta (1 with sequence 3 at 1.5T, 1 at 3T, and 1 at 7T).

After exclusion of the aortic segments with non-diagnostic quality, 134 segments remained for further analysis.

### 3.2 | Intraobserver analysis

Bland-Altman plots (Figure 2) for the intraobserver analysis showed good agreement of all parameters with low bias and narrow 95% CI for the difference of the two assessments by the same observer (forward flow volume:  $-18.4; 14.6$  mL; WSS:  $-0.17; 0.18$   $\text{N}/\text{m}^2$ ; peak velocity:  $-0.15; 0.10$  m/s). Also, no clear systematic pattern, for example, increasing or decreasing variability with higher averages, was observed so that sufficient agreement was concluded across the whole range of outcomes.

### 3.3 | Interobserver analysis

Agreement between the two observers was excellent for forward flow volume (ICC = 0.93), WSS (ICC = 0.93), and

peak velocity (ICC = 0.99). Bland-Altman analyses showed small biases and narrow CI (see Figure 3).

### 3.4 | Comparison of field strengths

The Bland-Altman analyses of the comparisons of field strengths showed differences in measurements in each pairwise comparison. These differences deviated from zero. No systemic pattern, for example, no increasing or decreasing variability with higher averages, was observed. However, equivalence between field strengths could not be concluded as the 95% CI of differences of measurements between field strength exceeded the range of the intraobserver variability (Table 3A and Figure 4A-C). When exclusively evaluating

the ascending aorta, the numbers only deviated slightly (Table 3A and Figure 4D-F).

Significant differences were found between 1.5T (sequence 1) and 3T as well as 3T and 7T for forward flow ( $P < .001$ ). No difference between 1.5T (sequence 1) and 7T was detected with respect to forward flow ( $P = .74$ ); however, the results of sequence 2 at 1.5T and 7T showed a significant difference ( $P < .001$ ). When comparing only the ascending aorta, forward flow volumes also differed significantly between 7T and sequence 1 at 1.5T ( $P < .001$ ). There was a significant difference in WSS between 1.5T (sequence 1) and 3T ( $P < .05$ ) and no differences between 3T and 7T ( $P > .2$ ) or between 1.5T and 7T with either sequence 1 or 2 ( $P > .3$ ). When analyzing only the ascending aorta, also 7T and 1.5T (sequence 1 and 2) differed significantly ( $P < .05$ ). There was

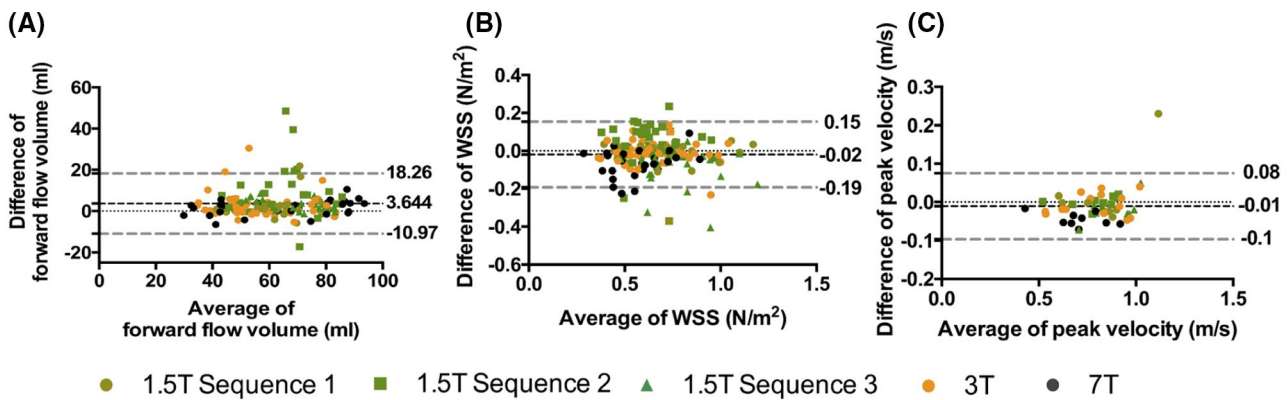


**FIGURE 3** Bland Altman analyses for interobserver analysis of forward flow volume (A), WSS (B), and peak velocity (C). Each field strength is coded in a different color. The three sequences at 1.5T are additionally coded using a different shape

**TABLE 3** 95% CI (confidence intervals) of differences of measurements of forward flow, WSS, and peak velocity for the comparison of field strengths (A) and sequences (B)

	Forward flow (mL)	WSS (N/m <sup>2</sup> )	Peak velocity (m/s)
<b>(A) 95% CI of differences of measurements</b>			
1.5T vs. 3T Whole aorta	-14.29-29.05	-0.21-0.27	-0.23-0.27
Ascending aorta only	-15.77-34.76	-0.17-0.27	-0.15-0.26
1.5T vs. 7T Whole aorta	-50.97-34.6	-0.25-0.29	*
Ascending aorta only	-57.02-29.3	-0.19-0.27	-0.21-0.28
3T vs. 7T Whole aorta	-60.03-30.75	-0.2-0.15	*
Ascending aorta only	-72.3-25.79	-0.2-0.19	-0.15-0.12
<b>(B) 95% CI of differences of measurements</b>			
Sequence 1 vs. 2 Whole aorta	-21.42-27.4	-0.17-0.32	-0.34-0.28
Ascending aorta only	-21.88-36.65	-0.12-0.33	-0.31-0.27
Sequence 1 vs. 3 Whole aorta	-17.55-9.75	-0.26-0.09	-0.29-0.19
Ascending aorta only	-18.67-10.45	-0.23-0.11	-0.28-0.2
Sequence 2 vs. 3 Whole aorta	-27.27-13.31	-0.37-0.06	-0.14-0.11
Ascending aorta only	-36.17-13.18	-0.38-0.05	-0.17-0.13

\*At 7T too few values could be calculated for an unbiased analysis. As the evaluation of the ascending aorta only contained less values in all comparisons, the amount of values generated at 7T were comparable.

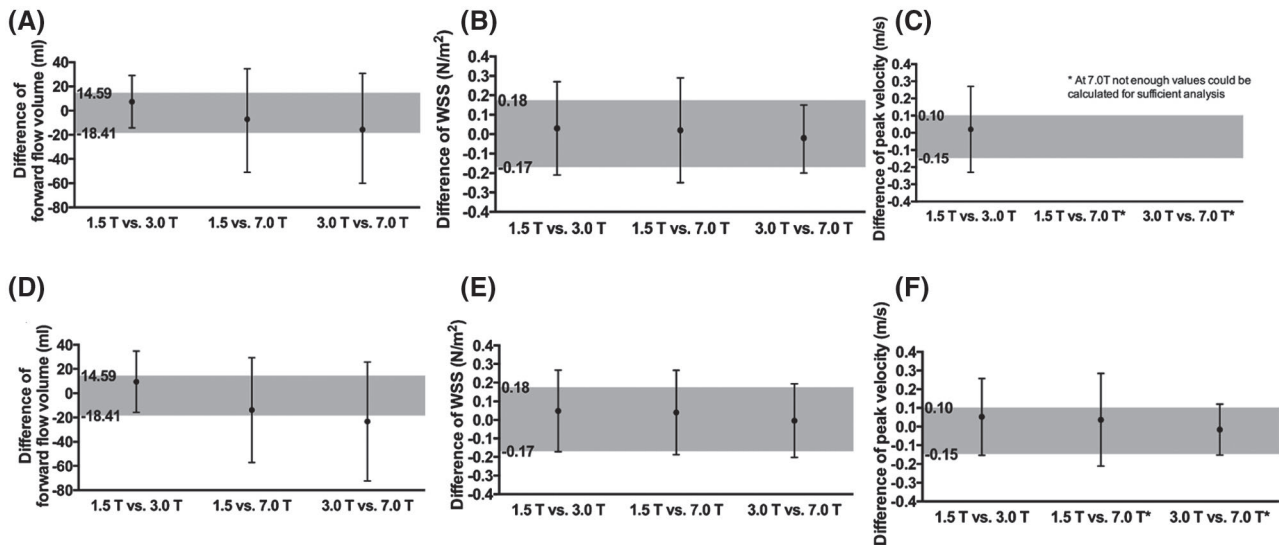


**FIGURE 4** Assessment of variability of differences of measurements by field strengths with respect to intraobserver variability for forward flow, WSS, and peak velocity for the whole aorta (A-C) and the ascending aorta only (D-F). The gray area displays the range of intraobserver variability (ie, 95% CI of the differences of intraobserver assessments [Bland-Altman approach]). Black dots indicate mean difference, while black bars indicate 95% CI of the difference between field strengths. As the evaluation of the ascending aorta only contained fewer values in all comparisons, the amount of values generated at 7T were comparable and, therefore, enough for sufficient analysis also in peak velocity

no significant difference in peak velocity between 1.5 (sequence 1) and 3T or 7T and no difference between 3T and 7T ( $P > .1$ ), but a significant difference between 1.5 (sequence 2) and 7T ( $P > .01$ ). This result remained in the analysis of the ascending aorta only.

The results remained the same when evaluating only the eight volunteers that could be examined at all field strengths.

There was a moderate positive correlation for forward flow between 1.5T (sequence 1) and 3T ( $r = 0.7$ ), and between 1.5T (sequence 1 and 2) and 7T ( $r = 0.5$ , respectively,  $r = 0.6$ ), as well as between 3T and 7T ( $r = 0.5$ ). For WSS, there was a moderate correlation between all field strengths (1.5T sequence 1 and 3T  $r = 0.7$ , 1.5T sequence 2 and 7T  $r = 0.7$ , 3T and 7T  $r = 0.7$ ), apart from 1.5T sequence 1 and 7T ( $r = 0.4$ ). Peak velocity correlated moderately between 1.5T (sequence 1) and 3T ( $r = 0.6$ ). At 7T, there were not enough values for a sufficient analysis (Figure 5).

### 3.5 | Comparison of sequences at 1.5T

The Bland-Altman analyses of the comparisons of sequences at 1.5T showed differences in measurements in each pairwise comparison. These differences deviated from zero. No systemic pattern, for example, no increasing or decreasing variability with higher averages, was observed. Equivalence between sequences could not be concluded for all parameters and comparisons apart from the comparison of forward flow volumes between sequence 1 and 3 as the 95% CI of differences of measurements by sequences exceeded the range of intraobserver variability (Table 3B and Figure 6A-C). When

exclusively evaluating the ascending aorta, the numbers only deviated slightly (Table 3B and Figure 6D-F).

Forward flow volume was found to be significantly different between sequences 1 and 3 and 2 and 3 ( $P < .001$ ), but did not differ significantly between sequence 1 and 2 ( $P > .1$ ). When comparing only the ascending aorta, forward flow volumes differed significantly between all sequences ( $P < .005$ ). There was a significant difference between all three sequences in WSS ( $P < .001$ ). These results remained when analyzing the ascending aorta only. Peak velocity did not differ significantly between any of the sequences ( $P > .5$ ), neither when analyzing the whole aorta nor when analyzing the ascending aorta only. These results remained the same when evaluating only the eight volunteers, that could be examined at all field strengths.

There was a moderate positive correlation for forward flow volume between sequences 1 and 2 ( $r = 0.5$ ) and sequences 2 and 3 ( $r = 0.7$ ) and a strong correlation between sequences 1 and 3 ( $r = 0.9$ ). For WSS, there was a moderate correlation between sequences 1 and 2 ( $r = 0.6$ ) and a strong correlation between sequences 1 and 3 ( $r = 0.8$ ) and between sequences 2 and 3 ( $r = 0.75$ ). Peak velocity correlated moderately between sequences 1 and 3 ( $r = 0.6$ ) and strongly between sequences 2 and 3 ( $r = 0.9$ ) (Figure 5).

## 4 | DISCUSSION

In this study, 4D flow data from three different sequences at 1.5T, one sequence at 3T, and one sequence at 7T were successfully acquired. The resulting images showed sufficient quality that allowed further analysis, despite challenges

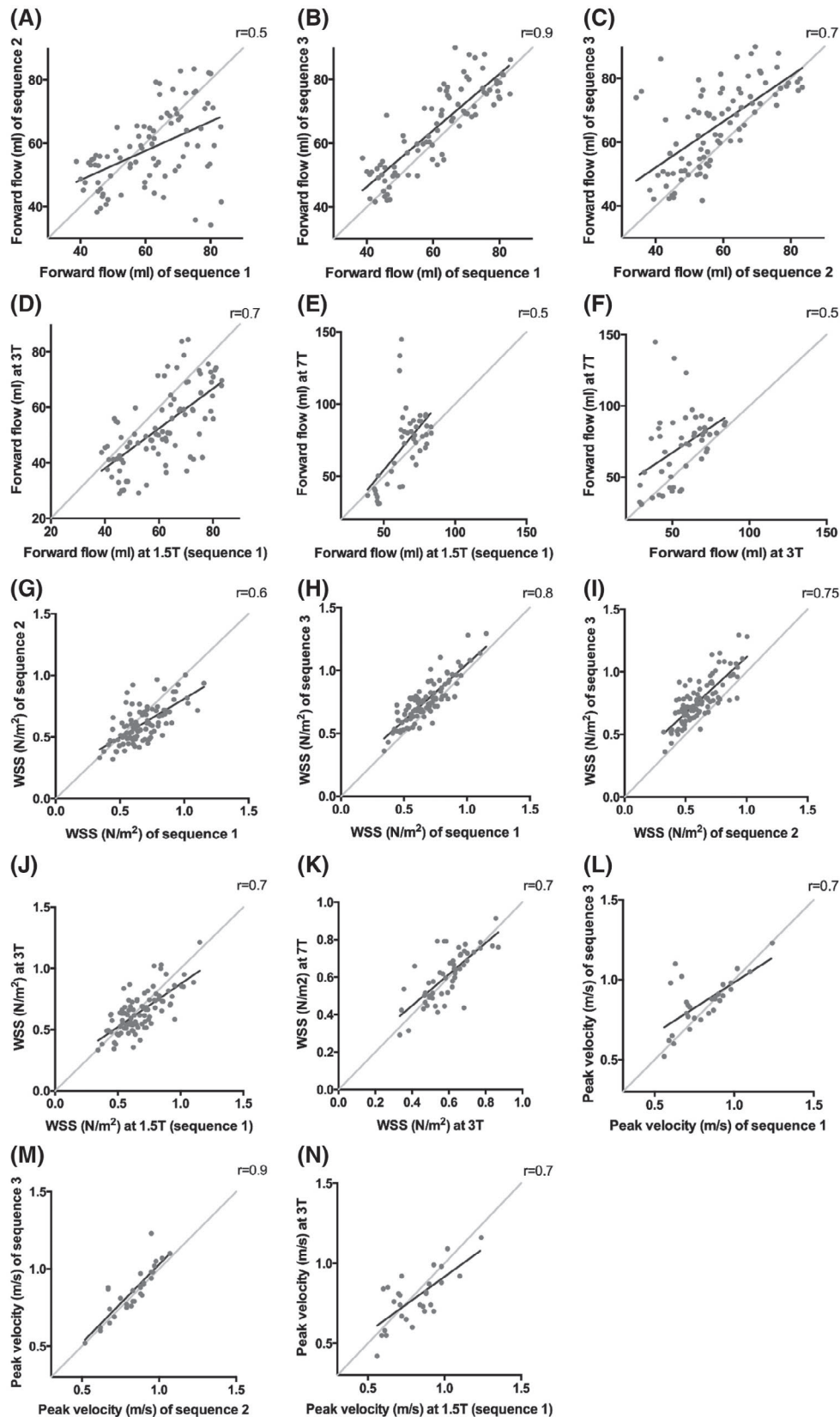


**FIGURE 5** Moderate to strong correlation between all sequences and field strengths for all parameters: correlation of forward flow for all sequences (A-C), correlation of forward flow for all field strengths (D-F), correlation of WSS for all sequences (G-I), correlation of WSS for field strengths (J,K), correlation of peak velocity for sequences (L,M), and correlation of peak velocity between 1.5 and 3T (at 7T not enough values for sufficient analysis) (N)



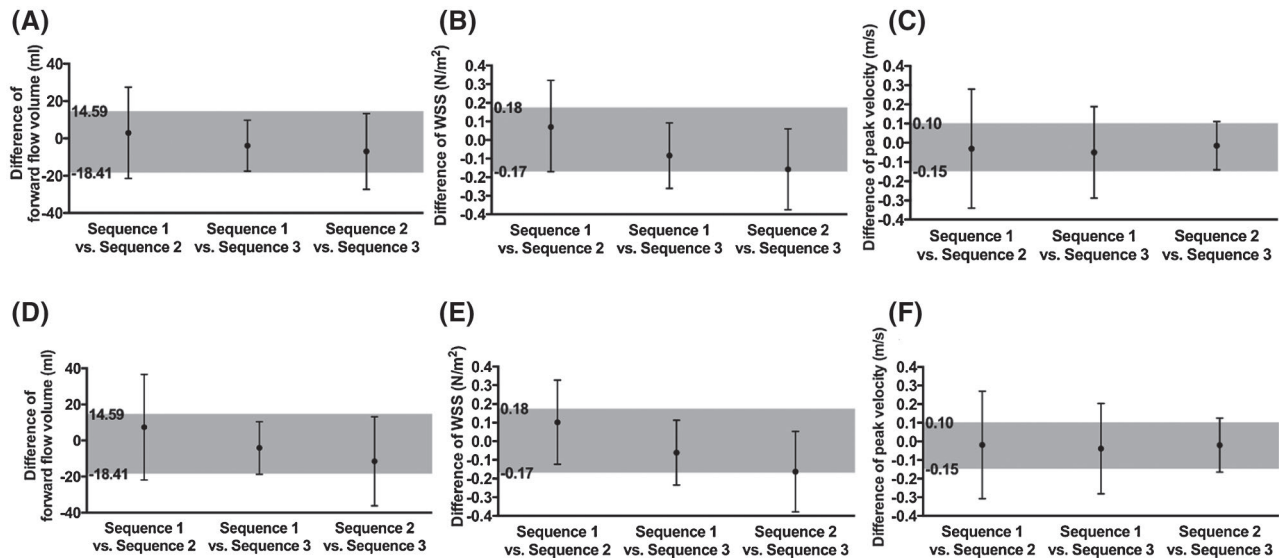


**FIGURE 6** Assessment of variability of differences of measurements by sequences at 1.5 T with respect to intraobserver variability for forward flow, WSS, and peak velocity for the whole aorta (A-C) and the ascending aorta only (D-F). The gray area displays the range of intraobserver variability (ie, 95% CI of the differences of intraobserver assessments (Bland-Altman approach)). Black dots indicate mean difference, while black bars indicate 95% CI of the difference between sequences

particularly related to the navigator, the positioning, the ECG, and coil placement at 7T. None of the tested sequences provided results that were equivalent with regard to the intraobserver variability in all parameters and significant differences were revealed. However, some comparisons suggest equivalence and some do not reveal any significant differences (Supporting Information Table S1).

Clinically, the impact of field strengths or sequences on the result is essential for follow-up investigations of a patient since a biased result can lead to a misdiagnosis. By calculating the equivalence, only the existence and amount of a potential bias can be identified, but the chance of misdiagnosing a patient with a certain pathology cannot be determined. For this evaluation, a tolerance range based on a comparison between healthy volunteers and patients with this certain pathology would be required, and the analysis needs to be performed again if the pathology of interest changes. As a first step, we retrospectively investigated data published in a previous study,<sup>9</sup> where we compared patients with aortic stenosis to healthy volunteers. In this former study, we showed a significant difference between healthy volunteers and patients with aortic stenosis in WSS and an increasing WSS with increasing severity of the stenosis. We re-used the data from this previous publication for a WSS comparison between patients with aortic stenosis (data of the previous study) and healthy subjects (data of the current study). This initial analysis showed that the differences in WSS between healthy volunteers and patients with severe aortic stenosis were larger than the differences in WSS between sequences/field strengths. However, this statement is not generally valid for patients with mild or moderate stenosis, a patient group

of high interest as they are typically diagnosed in this stage. Therefore, such patients could be misdiagnosed if the sequence or field strength changes in follow-up examinations.

Intra- and interobserver analysis show good agreement with low bias and narrow CI. In forward flow volume bias is lower in intraobserver analysis than in interobserver analysis, as expected. However, the 95% confidence interval is slightly larger in intraobserver analysis than in interobserver analysis. In the Bland-Altman plot of the intraobserver analysis, five outliers can be seen. These outliers are all from data acquired at 7T. An explanation for this might be given by insufficient flip angles, which was particularly observed in the descending aorta. Due to the low flip angles, the signal-to-noise ratio (SNR) decreases and might influence the delineation. In WSS, bias is also lower in intraobserver analysis than in interobserver analysis and the CI is similar. Only in peak velocity bias is lower in interobserver analysis than intraobserver analysis. The 95% CI is also slightly larger in interobserver analysis than in intraobserver analysis. However, both show excellent agreement. Peak velocity is measured in three areas of the aorta, and the highest velocity in each of the areas is given. Slight changes in placing the areas can lead to these slight changes in numbers.

#### 4.1 | Image quality

The lowest diagnostic quality was found at 7T, mainly in the aortic arch and the descending aorta. This seems to contradict the expected higher SNR at 7T in comparison to 3T or 1.5T. Indeed, Hess et al showed a higher SNR up to 2.2 times for

4D flow in the aorta at 7T compared with 3T.<sup>29</sup> In 4D flow in intracranial vessel imaging, a higher SNR at 7T compared with 3T resulted in a better delineation of small vessels and improved flow visualization.<sup>30</sup> The low image quality at 7T in our study was most likely caused by systematically low flip angles generated by the single-channel transmit coil within the arch and descending aorta that resulted in lower contrast. Modifying the hardware of the coil to specifically target the aorta and not the heart (as in the present study) or using a multi-transmit-channel coil combined with radiofrequency shimming could help solving this problem.

The one segment with non-diagnostic quality in sequence 1 at 1.5T was most likely due to a poorly positioned field of view during acquisition.

## 4.2 | Comparison of field strengths

The potential impact of field strength on the determination of hemodynamic parameters using 4D flow has been investigated before. Strecker et al did not find significant differences in the thoracic aorta of healthy volunteers between 1.5T and 3T.<sup>31</sup> However, they compared different 4D flow-derived parameters at 1.5 and 3T, while we further included 7T data as well as different sequences. In agreement with Strecker et al, we found a good agreement between quantitative analyses with similar values for flow volumes, peak velocities, and WSS.<sup>31</sup> In addition, we investigated if these aortic hemodynamic parameters obtained using the different sequences/field strengths were similar enough to be interchangeable. Therefore, we also evaluated equivalence, which could also be interpreted as a tolerance range according to a clinical perspective. Indeed, given the current lack of standardization, it is crucial to foster the clinical use of 4D flow MRI, to establish if sequences/field strengths can be changed for a patient's follow-up investigation without affecting results.

Significant differences were found in our cohort in the comparison of forward flow volumes, WSS, and peak velocity between different field strengths. However, not all comparisons were significantly different: Peak velocity did not differ significantly between 1.5T and 3T as well as 3T and 7T, and the comparison of the results obtained at 3T and 7T could even be considered equivalent with respect to the intraobserver variability in the ascending aorta only. Due to the limited number of datasets for peak velocity at 7T, this conclusion is limited and applies to the ascending aorta only.

Although some comparisons concerning the WSS did not show a significant difference, they exceeded the limits of intraobserver variability and were, therefore, not found to be equivalent. In forward flow, significant differences were found and the respective comparisons between field strengths exceeded the limits of intraobserver variability (Supporting Information Table S1). As in clinical evaluation, differences

in results can lead to a different diagnosis, these differences between field strengths should be taken into account. However, our findings suggest that peak velocity is less dependent on the field strength than WSS and forward flow.

## 4.3 | Comparison of sequences

Apart from the comparison of forward flow between sequence 1 and sequence 3, none of the compared parameters were equivalent with regard to the intraobserver variability.

The intraobserver variability was determined by analyzing a subset of examinations at all field strengths twice. An additional intraobserver analysis consisting only of examinations at 1.5T revealed a smaller variability resulting in a narrower range of equivalence. A closer look at the comparison of forward flow volumes between sequence 1 and 3 showed that they indeed lay within the range determined by intraobserver variability of all field strengths, but not within the range determined only by intraobserver variability at 1.5T. The comparison of peak velocity between sequence 2 and 3 only slightly exceeded the range of equivalence determined by intraobserver variability of all field strengths. Furthermore, it lay just within the range of equivalence determined by intraobserver variability at 1.5T only. These sequences might, therefore, be equivalent, however, only regarding peak velocity.

Significant differences were found in our cohort in the comparison of forward flow volumes, WSS, and peak velocity between sequences, although not between all parameters in all sequences. For the comparisons of forward flow and WSS significant differences were found. This was supported by the finding of the test for equivalence in these comparisons, as no equivalence between the sequences could be shown there either. In peak velocity, no significant difference was found. As the test for equivalence also already showed only a slight divergence, peak velocity seems to be the parameter least dependent on the type of sequence used.

As sequence 2 and 3 have identical acquisition parameters and differ only in the way of gating (prospectively vs. retrospectively), only minor difference between both sequences could be expected. However, they also show significant differences in forward flow and WSS. Only the comparison of peak velocity shows no significant differences and was found to be equivalent. Differences in forward flow may be explained by the different way of gating applied in sequence 2 and 3. Prospectively gated sequences do not cover the whole heart beat, but miss milliseconds of the diastolic phase, while retrospectively gated sequences cover the entire cardiac cycle. Therefore, differences can be expected already in healthy volunteers, as we showed. This difference is of even higher importance when examining patients with pathologies that affect the diastolic phase of the heart cycle (eg, aortic valve regurgitation). WSS, however, is

measured around peak systolic phase, which cannot be explained by the differences in gating. Interestingly, our data reflect that also WSS differs significantly between sequence 2 and 3, which motivates further investigations on the impact of triggering on derived WSS values.

A moderate to strong positive correlation was found for the comparison of all parameters in all sequences as well as in all field strengths. This means that 4D flow can be used and evaluated in all sequences and at all field strengths with reasonable results. Although the results of the different field strengths and sequences might not be interchangeable, the positive correlation also implies that a transfer might be possible with the establishment of a z-score.<sup>32</sup>

So far, 4D flow MRI been applied using various sequence types and at different field strengths. In clinical studies, it has been used at 1.5T<sup>11,15,18,33,34</sup> and 3T<sup>9,12-14,35,36</sup> or at both clinical field strengths.<sup>16,19,20,37-39</sup> Furthermore, 4D flow MRI has been evaluated at 7T.<sup>29,40</sup> Sequence characteristics ranged from echo time 2.2 to 6.1 ms, echo spacing 4.2 to 6.4 ms, spatial resolution 1.6-4 × 1.5-4 × 2.5-4 mm<sup>3</sup>, and ECG gating was performed either prospectively or retrospectively.<sup>13,16,18,36,37</sup> The impact of technical parameters of hemodynamic parameters of 4D flow sequences was also studied by other groups. Carlsson et al compared two 4D flow sequences to determine flow volumes in the whole heart with different acceleration techniques at 1.5T and 3T in healthy volunteers. They found significant differences between both sequences regarding peak blood flow.<sup>41</sup> The influence of different acceleration techniques on 4D flow was also analyzed in a whole heart study<sup>42</sup> and in brain vasculature<sup>43</sup>: Garg et al examined 25 volunteers as well as a thoracic phantom with three intracardiac 4D flow sequences with different acceleration techniques. They compared peak velocity and flow volume at the mitral and aortic valve of each 4D sequence. All results obtained by 4D flow sequences correlated well with those obtained by a slice-selective acquisition, but they correlated differently, with one sequence correlating excellently.<sup>42</sup> Sekine et al examined 16 volunteers with two accelerated 4D flow sequences and one non-accelerated sequence in brain vessels. They measured peak velocity and flow volume. Both accelerated scans agreed well with the non-accelerated sequence. They both underestimated peak velocity and flow volumes in some subjects, but in different vessels.<sup>43</sup> Montalba et al could show that spatial and temporal resolution had an impact on the measurement of flow volumes and peak velocity using 4D flow MRI in an aortic phantom.<sup>44</sup>

These studies show that different technical parameters of 4D flow sequences might have an impact on certain clinically important parameters. Clinically used sequences often differ slightly to one another, which might influence the result.

The differences between 4D flow at different field strengths could also be caused by physiological changes of hemodynamics and/or fluid or food intake<sup>45</sup> of the individual

volunteer, as our volunteers did not fast before conducting the scan. However, all scans were performed at approximately the same time of day resulting in a probable similar food influence on hemodynamics. All scans at 1.5T were performed in one scan without break, which implies a similar impact of food intake on hemodynamics over the whole scan.

Kamphuis et al tested scan-rescan reproducibility of an intracardiac 4D flow sequence. They showed a good reproducibility of 4D flow with good to strong correlation coefficients, depending on the evaluation method.<sup>46</sup> Stoll et al showed similar results in their study of intracardiac 4D flow scan-rescan assessment.<sup>36</sup> This shows that scan-rescan reproducibility for 4D flow is high, which suggests that the effect of changes in hemodynamics between the scans should be small and cannot fully explain the differences we found.

#### 4.4 | Limitations

This study was based on a limited number of healthy volunteers, and no phantom studies were performed. For the establishment of normal values, larger cohorts are needed. Acquisition parameters of the sequences at the different field strengths differ slightly, which is mainly caused by the availability of sequences and the hardware (eg, gradients) at the different scanners, but the parameters reflect the clinical setting.

Scan-rescan variability was not tested in this study, and differences here might also contribute to our findings. Comparison to other studies, however, showed smaller scan-rescan variability than the differences between field strengths/sequences found in our study.

No reference measurement such as 2D phase contrast imaging in selected planes was obtained based on which the LV stroke volume was calculated and compared with the volumes measured by 4D flow imaging. To assess a possible over- or underestimation of flow values, this is of interest for further investigations.

Furthermore, the results for the peak WSS shown in Figure 6 might be biased by the different reconstructed temporal resolution for the retrospective and prospective acquisitions at 1.5T. Since here five cardiac phases at peak systole are selected for both reconstruction types, the resulting interval is shorter for the retrospective scan, which may explain higher WSS values for this acquisition.

## 5 | CONCLUSIONS

Despite challenges particularly related to the navigator, the positioning, the ECG and coil placement at 7T, data from all sequences have been successfully acquired and resulting images showed sufficient quality that allowed further analysis. The hemodynamic results in this study showed agreement, as

the differences were found to be around zero with a certain variability, but were not found to be equivalent with regard to limits assessed by the intraobserver variability. In our view, this agreement was sufficient for a more detailed evaluation of the differences. The comparison of different hemodynamic parameters between the sequences, respectively, field strengths showed significant differences. Hence, field strength and/or different sequence acquisition parameters of one sequence might have an influence on 4D flow quantitative aortic hemodynamic parameters; therefore, equivalence between these parameters cannot be taken for granted, but should be verified before interpreting results and when conducting longitudinal or cross-center studies.

## ACKNOWLEDGMENTS

We thank all the volunteers for participation in the study. We also sincerely acknowledge the support of our MR technicians Denise Kleindienst, Kerstin Kretschel, Evelyn Polzin, and Martina Kohla, as well as our study nurses Annette Köhler-Rohde and Elke Nickel-Szczeczek in conducting all study scans. We thank Thomas Hadler for his help in editing the manuscript.

## CONFLICT OF INTEREST

Ning Jin and Andreas Greiser are full-time employees of Siemens Healthineers.

## ORCID

Sebastian Schmitter  <https://orcid.org/0000-0003-4410-6790>

Jeanette Schulz-Menger  <https://orcid.org/0000-0003-3100-1092>

## REFERENCES

1. Markl M, Chan FP, Alley MT, et al. Time-resolved three-dimensional phase-contrast MRI. *J Magn Reson Imaging*. 2003;17:499-506.
2. Wigstrom L, Sjoqvist L, Wranne B. Temporally resolved 3D phase-contrast imaging. *Magn Reson Med*. 1996;36:800-803.
3. Kim WY, Walker PG, Pedersen EM, et al. Left ventricular blood flow patterns in normal subjects: A quantitative analysis by three-dimensional magnetic resonance velocity mapping. *J Am Coll Cardiol*. 1995;26:224-238.
4. van Ooij P, Potters WV, Nederveen AJ, et al. A methodology to detect abnormal relative wall shear stress on the full surface of the thoracic aorta using four-dimensional flow MRI. *Magn Reson Med*. 2015;73:1216-1227.
5. Baumgartner H, Falk V, Bax JJ, et al. 2017 ESC/EACTS guidelines for the management of valvular heart disease. *Eur Heart J*. 2017;38:2739-2791.
6. Erbel R, Aboyans V, Boileau C, et al. 2014 ESC Guidelines on the diagnosis and treatment of aortic diseases: Document covering acute and chronic aortic diseases of the thoracic and abdominal aorta of the adult. The task force for the diagnosis and treatment of aortic diseases of the European Society of Cardiology (ESC). *Eur Heart J*. 2014;35:2873-2926.
7. Lorenz R, Bock J, Barker AJ, et al. 4D flow magnetic resonance imaging in bicuspid aortic valve disease demonstrates altered distribution of aortic blood flow helicity. *Magn Reson Med*. 2014;71:1542-1553.
8. Barker AJ, Markl M, Burk J, et al. Bicuspid aortic valve is associated with altered wall shear stress in the ascending aorta. *Circ Cardiovasc Imaging*. 2012;5:457-466.
9. von Knobelsdorff-Brenkenhoff F, Karunaharamoorthy A, Trauzeddel RF, et al. Evaluation of aortic blood flow and wall shear stress in aortic stenosis and its association with left ventricular remodeling. *Circ Cardiovasc Imaging*. 2016;9:e004038.
10. van der Palen RL, Barker AJ, Bollache E, et al. Altered aortic 3D hemodynamics and geometry in pediatric Marfan syndrome patients. *J Cardiovasc Magn Reson*. 2017;19:30.
11. Rodriguez-Palomares JF, Dux-Santoy L, Guala A, et al. Aortic flow patterns and wall shear stress maps by 4D-flow cardiovascular magnetic resonance in the assessment of aortic dilatation in bicuspid aortic valve disease. *J Cardiovasc Magn Reson*. 2018;20:28.
12. Sherrah AG, Callaghan FM, Puranik R, et al. Multi-velocity encoding four-dimensional flow magnetic resonance imaging in the assessment of chronic aortic dissection. *Aorta (Stamford, Conn)*. 2017;5:80-90.
13. Bissell MM, Loudon M, Hess AT, et al. Differential flow improvements after valve replacements in bicuspid aortic valve disease: A cardiovascular magnetic resonance assessment. *J Cardiovasc Magn Reson*. 2018;20:10.
14. Stephens EH, Hope TA, Kari FA, et al. Greater asymmetric wall shear stress in Sievers' type 1/LR compared with 0/LAT bicuspid aortic valves after valve-sparing aortic root replacement. *J Thorac Cardiovasc Surg*. 2015;150:59-68.
15. Hope MD, Sigovan M, Wrenn SJ, Saloner D, Dyverfeldt P. MRI hemodynamic markers of progressive bicuspid aortic valve-related aortic disease. *J Magn Reson Imaging*. 2014;40:140-145.
16. van Ooij P, Markl M, Collins JD, et al. Aortic valve stenosis alters expression of regional aortic wall shear stress: New insights from a 4-dimensional flow magnetic resonance imaging study of 571 subjects. *J Am Heart Assoc*. 2017;6:e005959.
17. von Knobelsdorff-Brenkenhoff F, Trauzeddel RF, Barker AJ, Gruettner H, Markl M, Schulz-Menger J. Blood flow characteristics in the ascending aorta after aortic valve replacement—a pilot study using 4D-flow MRI. *Int J Cardiol*. 2014;170:426-433.
18. Trauzeddel RF, Lobe U, Barker AJ, et al. Blood flow characteristics in the ascending aorta after TAVI compared to surgical aortic valve replacement. *Int J Cardiovasc Imaging*. 2016;32:461-467.
19. Geiger J, Hirtler D, Gottfried K, et al. Longitudinal evaluation of aortic hemodynamics in Marfan syndrome: New insights from a 4D flow cardiovascular magnetic resonance multi-year follow-up study. *J Cardiovasc Magn Reson*. 2017;19:33.
20. Bollache E, Fedak PWM, van Ooij P, et al. Perioperative evaluation of regional aortic wall shear stress patterns in patients undergoing aortic valve and/or proximal thoracic aortic replacement. *J Thorac Cardiovasc Surg*. 2018;155:2277-2286.e2272.
21. Ma LE, Markl M, Chow K, et al. Aortic 4D flow MRI in 2 minutes using compressed sensing, respiratory controlled adaptive k-space reordering, and inline reconstruction. *Magn Reson Med*. 2019;81:3675-3690.
22. Bollache E, Barker AJ, Dolan RS, et al. k-t accelerated aortic 4D flow MRI in under two minutes: Feasibility and impact of resolution, k-space sampling patterns, and respiratory navigator gating on hemodynamic measurements. *Magn Reson Med*. 2018;79:195-207.

23. Thalhammer C, Renz W, Winter L, et al. Two-dimensional sixteen channel transmit/receive coil array for cardiac MRI at 7.0 T: Design, evaluation, and application. *J Magn Reson Imaging*. 2012;36:847-857.
24. Frauenrath T, Hezel F, Renz W, et al. Acoustic cardiac triggering: A practical solution for synchronization and gating of cardiovascular magnetic resonance at 7 Tesla. *J Cardiovasc Magn Reson*. 2010;12:67.
25. Prothmann M, von Knobelsdorff-Brenkenhoff F, Topper A, et al. High spatial resolution cardiovascular magnetic resonance at 7.0 Tesla in patients with hypertrophic cardiomyopathy—First experiences: Lesson learned from 7.0 Tesla. *PLoS One*. 2016;11:e0148066.
26. Potters WV, van Ooij P, Marquering H, vanBavel E, Nederveen AJ. Volumetric arterial wall shear stress calculation based on cine phase contrast MRI. *J Magn Reson Imaging*. 2015;41:505-516.
27. Walker PG, Cranney GB, Scheidegger MB, Waseleski G, Pohost GM, Yoganathan AP. Semiautomated method for noise reduction and background phase error correction in MR phase velocity data. *J Magn Reson Imaging*. 1993;3:521-530.
28. Rose MJ, Jarvis K, Chowdhary V, et al. Efficient method for volumetric assessment of peak blood flow velocity using 4D flow MRI. *J Magn Reson Imaging*. 2016;44:1673-1682.
29. Hess AT, Bissell MM, Ntusi NA, et al. Aortic 4D flow: quantification of signal-to-noise ratio as a function of field strength and contrast enhancement for 1.5T, 3T, and 7T. *Magn Reson Med*. 2015;73:1864-1871.
30. van Ooij P, Zwanenburg JJ, Visser F, et al. Quantification and visualization of flow in the Circle of Willis: Time-resolved three-dimensional phase contrast MRI at 7 T compared with 3 T. *Magn Reson Med*. 2013;69:868-876.
31. Strecker C, Harloff A, Wallis W, Markl M. Flow-sensitive 4D MRI of the thoracic aorta: Comparison of image quality, quantitative flow, and wall parameters at 1.5 T and 3 T. *J Magn Reson Imaging*. 2012;36:1097-1103.
32. Gautier M, Detaint D, Fermanian C, et al. Nomograms for aortic root diameters in children using two-dimensional echocardiography. *Am J Cardiol*. 2010;105:888-894.
33. van Kesteren F, Wollersheim LW, Baan J Jr, et al. Four-dimensional flow MRI of stented versus stentless aortic valve bioprostheses. *Eur Radiol*. 2018;28:257-264.
34. Rengier F, Delles M, Eichhorn J, et al. Noninvasive 4D pressure difference mapping derived from 4D flow MRI in patients with repaired aortic coarctation: Comparison with young healthy volunteers. *Int J Cardiovasc Imaging*. 2015;31:823-830.
35. Binter C, Gotschy A, Sundermann SH, et al. Turbulent kinetic energy assessed by multipoint 4-dimensional flow magnetic resonance imaging provides additional information relative to echocardiography for the determination of aortic stenosis severity. *Circ Cardiovasc Imaging*. 2017;10:e005486
36. Stoll VM, Loudon M, Eriksson J, et al. Test-retest variability of left ventricular 4D flow cardiovascular magnetic resonance measurements in healthy subjects. *J Cardiovasc Magn Reson*. 2018;20:15.
37. Garcia J, van der Palen RLF, Bollache E, et al. Distribution of blood flow velocity in the normal aorta: Effect of age and gender. *J Magn Reson Imaging*. 2018;47:487-498.
38. Geiger J, Rahsepar AA, Suwa K, et al. 4D flow MRI, cardiac function, and T1 -mapping: Association of valve-mediated changes in aortic hemodynamics with left ventricular remodeling. *J Magn Reson Imaging*. 2018;48:121-131.
39. Raghav V, Barker AJ, Mangiameli D, Mirabella L, Markl M, Yoganathan AP. Valve mediated hemodynamics and their association with distal ascending aortic diameter in bicuspid aortic valve subjects. *J Magn Reson Imaging*. 2018;47:246-254.
40. Schmitter S, Schnell S, Ugurbil K, Markl M, Van de Moortele PF. Towards high-resolution 4D flow MRI in the human aorta using kt-GRAPPA and B1+ shimming at 7T. *J Magn Reson Imaging*. 2016;44:486-499.
41. Carlsson M, Toger J, Kanski M, et al. Quantification and visualization of cardiovascular 4D velocity mapping accelerated with parallel imaging or k-t BLAST: Head to head comparison and validation at 1.5 T and 3 T. *J Cardiovasc Magn Reson*. 2011;13:55.
42. Garg P, Westenberg JJM, van den Boogaard PJ, et al. Comparison of fast acquisition strategies in whole-heart four-dimensional flow cardiac MR: Two-center, 1.5 Tesla, phantom and in vivo validation study. *J Magn Reson Imaging*. 2018;47:272-281.
43. Sekine T, Amano Y, Takagi R, Matsumura Y, Murai Y, Kumita S. Feasibility of 4D flow MR imaging of the brain with either Cartesian y-z radial sampling or k-t SENSE: Comparison with 4D Flow MR imaging using SENSE. *Magn Reson Med Sci*. 2014;13:15-24.
44. Montalba C, Urbina J, Sotelo J, et al. Variability of 4D flow parameters when subjected to changes in MRI acquisition parameters using a realistic thoracic aortic phantom. *Magn Reson Med*. 2018;79:1882-1892.
45. Hauser JA, Muthurangu V, Steeden JA, Taylor AM, Jones A. Comprehensive assessment of the global and regional vascular responses to food ingestion in humans using novel rapid MRI. *Am J Physiol Regul Integr Comp Physiol*. 2016;310:R541-R545.
46. Kamphuis VP, van der Palen RLF, de Koning PJH, et al. In-scan and scan-rescan assessment of LV in- and outflow volumes by 4D flow MRI versus 2D planimetry. *J Magn Reson Imaging*. 2018;47:511-522.

## SUPPORTING INFORMATION

Additional Supporting Information may be found online in the Supporting Information section.

**TABLE S1** Comparison of forward flow, WSS and peak velocity between field strengths (a) and sequences (b) in a color-coded three-scale metric combining both the statistical and the equivalence testing: Values indicated in red reflect differences in both tests and a change between the respective sequences/field strengths is not recommended. Yellow colored values denote a difference in only one of the tests, changes of sequences/field strengths can be done with careful consideration and keeping this bias in mind. Values in green indicate no differences in both tests, changes are possible. \* When comparing the results in the ascending aorta only, the color changes to red

**VIDEO S1** Streamlines of one volunteer's aorta at 1.5T (sequences 1-3), at 3T and at 7T

**How to cite this article:** Wiesemann S, Schmitter S, Demir A, et al. Impact of sequence type and field strength (1.5, 3, and 7T) on 4D flow MRI hemodynamic aortic parameters in healthy volunteers. *Magn Reson Med*. 2021;85:721-733.

<https://doi.org/10.1002/mrm.28450>